Tunneling magnetoresistance in phase-separated manganite nanobridges

G. Singh-Bhalla,[1,2] A. Biswas,[1] and A. F. Hebard[1,*]
[1]*Department of Physics, University of Florida, Gainesville, Florida 32611, USA*
[2]*Department of Physics, University of California, Berkeley, California 94720, USA*
(Received 28 May 2009; revised manuscript received 18 September 2009; published 15 October 2009)

The manganite $(La,Pr,Ca)MnO_3$ is well known for its micrometer-scale phase separation into coexisting ferromagnetic metallic (FMM) and insulating regions. Fabrication of bridges with widths smaller than the phase-separation length scale has allowed us to probe the magnetic properties of individual phase-separated regions. At the onset of phase separation, a magnetic field induced insulator-to-metal transition among a discrete number of domains within the narrow bridges gives rise to abrupt, low-field colossal magnetoresistance steps at well-defined switching fields. At lower temperatures when the FMM phase becomes energetically favorable, the insulating regions shrink to form thin insulating strips separating adjacent FMM regions with different coercive fields. Tunneling magnetoresistance is observed across the naturally occurring intrinsic insulating strips (tunnel barriers) spanning the width of the bridges. The presence of such intrinsic tunnel barriers introduces an alternative approach to fabricating novel nanoscale magnetic tunnel junctions.

DOI: 10.1103/PhysRevB.80.144410 PACS number(s): 75.47.Lx, 73.40.Gk, 75.60.Ch

I. INTRODUCTION

Driven in part by the potential for applications in the magnetic storage and memory industry, the ongoing quest for large low-field magnetoresistance has prompted the exploration of several types of insulating tunnel barriers. To date low-field magnetoresistance studies, which explore the usage of fields on the order of hundreds of Oersteds (Oe) to switch between high- and low-resistance states, have focused on transport across barriers such as grain boundaries in polycrystalline[1,2] or bicrystalline[3] films, and across thin-film insulators sandwiched between ferromagnetic metallic (FMM) electrodes in trilayer or multilayer configurations.[4] Utilizing an altogether different approach, we exploit the micrometer-scale intrinsic phase separation in $(La_{1-x}Pr_x)_{1-y}Ca_yMnO_3$ or LPCMO, with $x=0.5$ and $y=0.33$, which results from a competition between the FMM and insulating states with comparable free energies. Below the Curie temperature, LPCMO undergoes a phase change from an insulating state to a ferromagnetic metallic state. During the phase transition, LPCMO films become phase separated with the FMM regions growing in size within the insulating background until the sample is fully ferromagnetic at temperatures below about 50 K. When LPCMO thin films are reduced in dimensions to narrow bridges of width smaller than the individual phase regions, alternating insulating and FMM regions can form along the bridge length during phase separation. Below we show that within the phase-separation temperature range we observe low-field colossal magnetoresistance (LFCMR) across the length of the bridge when the insulating phase is dominant and tunneling magnetoresistance (TMR) when the ferromagnetic phase is dominant. The LFCMR results from a magnetic field induced insulator-to-metal (IM) transition among a discrete number of insulating regions along the bridge length while TMR is observed as a result of tunneling across insulating regions which separate FMM regions with different coercive fields.

Recent observations of discrete resistivity steps on narrow bridges of the mixed phase manganites $Pr_{0.65}(Ca_{0.75}Sr_{0.25})_{0.35}MnO_3$ and LPCMO provide evidence of alternating FMM and insulating regions spanning the full width of the structure.[5–8] In our own work on LPCMO bridges, we have shown evidence of temperature-independent direct tunneling across the intrinsic insulating regions separating FMM regions.[5] However, spin-polarized tunneling across such intrinsic insulating regions was not considered. Here we describe the explicit role of spin-polarized currents on magnetotransport in submicron structures where intrinsic insulating tunnel barriers[5] resulting from phase-separation dominate.

LPCMO with $x=0.5$ and $y=0.33$ exhibits properties characteristic of both parent compounds $La_{0.67}Ca_{0.33}MnO_3$ and $Pr_{0.67}Ca_{0.33}MnO_3$. LPCMO is paramagnetic insulating (PI) at room temperature and portions[9] of the sample undergo a martensitic-type[10] phase transition to an antiferromagnetic charge-ordered insulating (COI) phase below about 240 K (T_{CO}).[11,12] (In contrast, the parent compound $Pr_{0.67}Ca_{0.33}MnO_3$ fully transitions to the COI state.[13]) The remaining PI regions below T_{CO} have also been referred to as a strain-stabilizing charge-disordered insulating (CDI) phase.[14,15] Figure 1 shows a resistivity vs temperature curve of an unpatterned LPCMO thin film with vertical lines marking the transition temperatures and boundaries between the different phases.

Below the Curie temperature (150 K), small FMM islands emerge within the CDI regions. Upon further cooling below the insulator-to-metal transition temperature, $T_{IM}^0=105$ K, (the superscript denotes the transition temperature of unpatterned films[16]), the FMM regions begin to grow in size at the expense of the insulating phases. It has been proposed that the structural strain between the pseudocubic FMM phase and the Jahn-Teller distorted COI phase accommodates the strain-stabilizing CDI regions at the boundary.[14,15] At temperatures near the insulator-to-metal transition, the insulating and metallic phases have comparable free energies. Thus in this temperature range phase separation is dynamic such that the FMM and insulating regions are not pinned but evolve in shape and size with changing temperature, as confirmed by

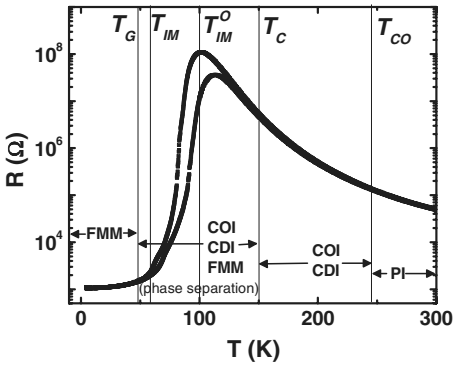

FIG. 1. Temperature-dependent resistivity of an unpatterned LPCMO thin film grown on $NdGaO_3$ (011) substrate. Vertical lines and labels identify the various phase-transition temperatures and boundaries discussed in the following sections. Beginning from the higher temperatures, T_{CO}=240 K marks the approximate charge-ordering temperature (values vary in the literature), T_C marks the Curie temperature, T^0_{IM}=105 K marks the onset of large-scale phase separation and the maximum of the resistivity peak for unpatterned thin films, T_{IM}=64 K marks the onset of a stable ferromagnetic state (a metastable insulating state) and the maximum of the resistivity peak for the patterned submicron bridges, and lastly T_G=48 K marks the fully ferromagnetic metallic state of the sample.

transmission electron microscopy magnetic imaging[17,18] and time-dependent relaxation measurements of resistivity.[11] Finally, cooling below what is often referred to as the blocking[11] or glass transition[12] temperature T_G, (with $T^0_{IM} > T_G$ as labeled in Fig. 2), the sample is predominantly in a single-phase ferromagnetic state[19] characterized by long relaxation-time constants.

It is within the phase coexistence temperature range, $T^0_{IM} > T > T_G$, that we observe the anisotropic, LFCMR, and

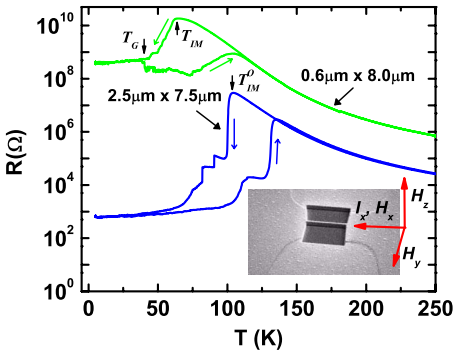

FIG. 2. (Color online) Temperature-dependent resistance for both cooling and warming (indicated by arrows) of a 2.5-μm-wide bridge (blue, lower curve) and a 0.6-μm-wide bridge (green, upper curve) patterned from 30-nm-thick LPCMO thin films reveal the evolution of pronounced steplike changes and the insulator-to-metal transition temperature (see text) as the bridge width becomes comparable to (2.5 μm) and then smaller than (0.6 μm) the micron-size regions of coexisting COI and FMM phases. A scanning electron micrograph of a 0.2-μm-wide bridge [with the protective polymer and metal layers still present (Ref. 5)] taken shortly after the FIB process is shown in the inset together with the orientations of the applied fields: H_x, H_y, or H_z.

TMR effects in the submicrometer wide bridges. Since the CDI regions are metastable with respect to a ferromagnetic state, a much smaller magnetic field is required for an insulator-to-metal transition than for the COI phase. In this way, as discussed below, it is possible to distinguish the effect of each phase on the measured magnetoresistance.

II. EXPERIMENT

To fabricate the bridges, we first deposited single-crystalline, epitaxial, 30-nm-thick LPCMO films with x=0.5 and y=0.33 on heated (820°C) $NdGaO_3$ (110) substrates using pulsed laser deposition.[19] $NdGaO_3$ (NGO) substrates, which are orthorhombic with a slight anisotropy along the (011) plane, induce a slight tensile strain on the LPCMO thin films.[20] Next, using a combination of photolithography and a focused ion beam (FIB), bridges ranging from 100 nm to 1 μm in width were fabricated.[5] A scanning electron microscopy image of a 0.2-μm-wide bridge is shown in Fig. 2, inset. Pressed indium dots and gold wire were used to make contacts. Resistance (R) measurements were made by sourcing +/−1 nA dc and measuring voltage. A magnetic field was applied three consecutive times at each temperature along three directions H_z, H_x, and H_y with respect to the current flow I_x as depicted in Fig. 2, and ramped at 25 Oe/s.

III. RESULTS AND DISCUSSION

A. Temperature-dependent resistance of LPCMO bridges

A systematic reduction in bridge width starting at 5.0 μm revealed no significant changes in $R(T)$ compared to the unpatterned thin films down to 2.5 μm, below which, as shown in Fig. 2 (lower, blue curve), small steps accompanying the IM transition (for $T < T^0_{IM}$=105 K) begin to appear since the bridge width is now on the order of the individual phase regions.[6] T^0_{IM} however, remains the same for the 2.5 μm bridge (shown) as for the unpatterned thin films.[5,16] Significant deviations in the resistance are observed for bridges of width less than 0.9 μm, where in most cases the insulator-to-metal transition temperature (T_{IM}=64 K for the 0.6-μm-wide bridge) shifts to a lower value (Fig. 2, upper green curve). We attribute this shift to dimensionally limited percolation from two dimensional to one dimensional, though we cannot fully rule out the effect of disorder introduced during the fabrication process. A high-resistance temperature-independent state begins to appear below T_G =48 K.

Here we discuss data in the microscale phase-separation temperature range $T^0_{IM} > T > T_G$ for a 0.6-μm-wide bridge[5] with magnetoresistance properties that are typical of bridges we have fabricated below 0.9 μm in width. At the onset of phase separation the sample is predominantly insulating with emerging FMM islands which grow with decreasing temperature. In this temperature range, anisotropic LFCMR is observed across the predominantly insulating samples. The effect is most prominent for $T^0_{IM} > T > T_{IM}$. Below T_{IM}, for $T_{IM} > T > T_G$ the FMM phase becomes dominant while the insulating phases shrink further. In this temperature range,

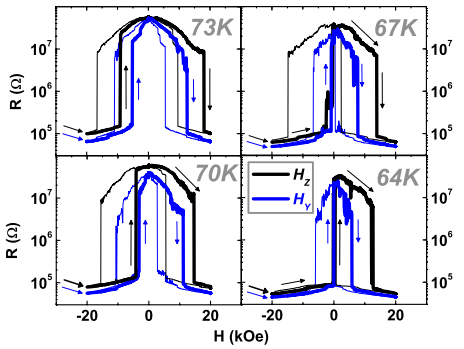

FIG. 3. (Color online) For temperatures, $T > T_{IM}$ for the 0.6-μm-wide bridge, repeated magnetic field sweeps at the indicated temperatures (73, 70, 67, and 64 K) reveal reproducible hysteretic temperature-dependent colossal resistance jumps that are more sensitive to in-plane (H_x,H_y) rather than perpendicular (H_z, black lines) fields. The critical switching field from high to low resistance reduces with decreasing temperature.

TMR peaks are observed across the remnant insulating tunnel barriers and cease to exist for $T < T_G$ when any remaining insulating phase is metastable in an applied magnetic field. In the following sections, the magnetoresistance and the corresponding phase morphology is discussed in each of the three temperature ranges.

B. Magnetoresistance across the 0.6-μm-wide LPCMO bridge

1. Magnetoresistance for $T^0_{IM} > T > T_{IM}$ (LFCMR)

For temperatures above $T^0_{IM}=105$ K during the cooling cycle, the sample is in a predominantly insulating state with nanoscale FMM phase fluctuations (i.e., small compared to the bridge width). Thus before the onset of large-scale phase separation above 105 K, the MR curves are no different from those observed for unpatterned thin films[19] for fields $\leq$ 20 kOe and are thus not discussed here. For $T^0_{IM} > T > T_{IM}$ however, we observe (Fig. 3) colossal (100-fold) field-induced resistance changes at well-defined anisotropic switching fields. The temperature range for these large resistance changes coincides with the maximum CMR effect in our unpatterned films. Here, the high-resistance values ($\approx 10^8$ Ω) correspond to limited conduction through insulating regions which with increasing field shrink to form remnant (lower resistance) tunnel barriers separating ferromagnetic regions. The insulating regions may not be fully removed for the 20 kOe fields shown in Fig. 3 since unpatterned thin-film resistivity is not achieved unless a field as high as 50 kOe is applied.

Comparison of our results with the parent compound $Pr_{0.67}Ca_{0.33}MnO_3$ suggest that with decreasing temperature, there is a reduction in the free energy of the FMM phase and the regions of insulating phase undergo a first-order phase transition to an FMM state, resulting in a concomitant colossal resistance drop.[13] In like manner a distribution of such first-order hysteretic transitions over many domains can account for the continuous field-induced phase transitions observed in unpatterned thin films of LPCMO (Ref. 19) as shown in Fig. 4 and in crystals of the parent compound

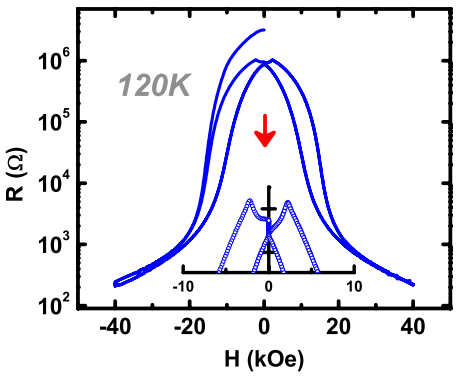

FIG. 4. (Color online) Unpatterned thin-film $R(H_y)$ data in the range $T_C > T = 120$ K $> T_{IM}$. The low- to high-field transitions shown expanded in the inset are smooth when compared to the bridge data in Fig. 3. A distribution of the first-order transitions shown in Fig. 3 over many domains may account for this.

$Pr_{0.67}Ca_{0.33}MnO_3$.[13] The sensitivity of the first-order phase transition to thermal fluctuations[13] is likely to be enhanced near T_{IM}, thus accounting for the unusual asymmetric transitions observed at the boundary temperature, $T_{IM}=64$ K, below which single irreversible colossal transitions to a predominantly FMM state occur (for example, see Fig. 5, $T=57$ K).

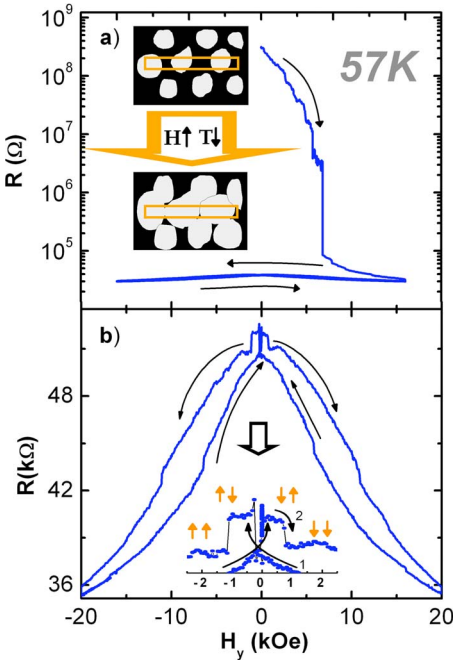

FIG. 5. (Color online) For the 0.6-μm-wide bridge, for temperatures above T_G and below T_{IM} magnetic field induced phase transitions terminate in a predominantly low-resistance FMM state that exhibits TMR. (a) A field-induced insulator-metal transition at 57 K of a zero-field-cooled sample showing a pronounced resistance drop at $H_z=6$ kOe and subsequent entrance into a low-resistance phase that is stable with respect to repeated field sweeps between ± 20 kOe. The inset schematically depicts the coalescence of FMM (white) regions at the expense of insulating (black) regions with applied fields or lowering temperatures, with a rectangular overlay depicting the 0.6 μm bridge. (b) Magnification of the TMR region, as described in the text.

As seen in Fig. 3, the field-induced changes in the 0.6-μm-wide bridge occur more readily for in-plane (H_y, blue curves) easy-axis fields,[21] than the out-of-plane fields along H_z. In thin-film ferromagnets, the demagnetization fields arising from shape anisotropy generally give rise to a greater sensitivity of the magnetization to in plane compared to out-of-plane applied fields. In our bridges, magnetoresistance is affected in the same way giving rise to the observed anisotropy in $R(H)$. With decreasing temperature the ferromagnetic regions increasingly fill the available volume of the film and the corresponding increase in the demagnetizing field results in increasingly anisotropic phase transitions as seen in Fig. 3. The magnetic anisotropy of the CMR effect manifests itself more dramatically in narrow bridges than in thin films, possibly due to the lack of numerous isotropic planar conduction paths in narrow bridges which are readily available in films.

2. Magnetoresistance for $T_{IM} > T > T_G$ (TMR)

Below T_{IM}, in the dynamic phase-separated state defined by $T_{IM} > T > T_G$,[11,12,18] the CDI and COI phases are metastable in applied magnetic fields as the FMM phase becomes energetically favorable, partially as a result of substrate-induced strain.[22] Figure 5(a) illustrates this effect at 57 K. Initially upon increasing H_y, $R(H_y)$ drops nearly 4 orders of magnitude and exhibits sharp steps[13,19] resulting from an incremental conversion of the insulating phases to FMM. The FMM regions increase in size and volume, separated by shrinking insulating regions along the bridge length.

Figure 5(b) (inset for 57 K) shows a magnified version of the low-resistance region. Here we note the distinct formation of low-field peaks (3.5% MR) indicating that the small amount of insulating phase present between the growing ferromagnetic region acts as a stable tunnel barrier. It is useful to compare regions of alternating insulating and FMM phases along the length of the narrow bridges to microscopic analogs of the insulating and FMM multilayers. Just as TMR is observed in such fabricated spin-polarized tunnel junctions, two resistance states are seen for field sweeps through zero field in each direction: a high-resistance state for antiparallel spin alignment ($\uparrow\downarrow$) and a low-resistance state for parallel alignment ($\uparrow\uparrow$). As noted in previous theoretical works,[23,24] TMR across coexisting insulating and FMM regions in phase-separated manganites may help explain some of the observed transport properties of bulk crystals. For instance, the low-field positive magnetoresistance when crossing $H=0$ Oe in $R(H)$ for unpatterned thin films (see inset of Fig. 4) may be a manifestation of TMR between ferromagnetic regions separated by COI tunnel barriers in unpatterned thin films.

The main panel of Fig. 6 shows the evolution of the low-field TMR with lowering temperature. For the cooling run shown in the inset of Fig. 6, TMR remained at nearly 10% for $48 < T < 52$ K. The TMR value is much smaller than the several 100% observed at low temperatures in manganite multilayers[21] and may reflect the fact that the ferromagnetic regions on either side of the intrinsic tunnel barrier may not be of uniform magnetization. Meanwhile, the integrity and shape of the intrinsic tunnel barrier as well as the possibility

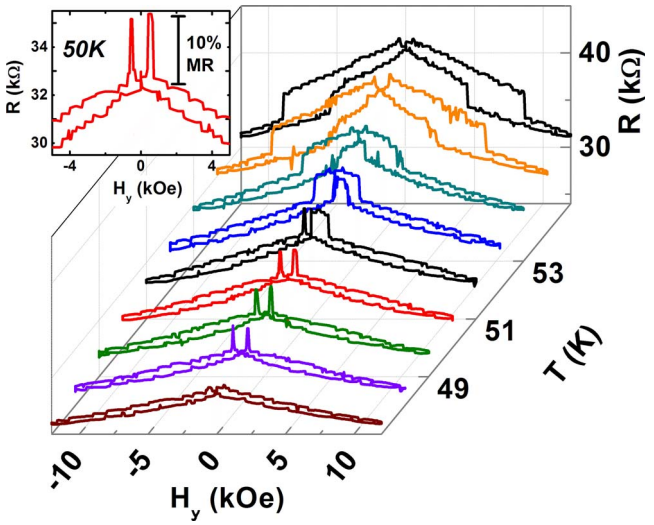

FIG. 6. (Color online) Waterfall plot of repeated magnetic field sweeps in the temperature range, $T_{IM} > T > T_G$, showing the temperature-dependent evolution of TMR peaks and their disappearance below $T_G = 48$ K.

of spin canting at the interface between the insulating and FMM regions can also play a significant role which cannot be determined from the measurements discussed here.

At higher temperatures (i.e., top three curves in Fig. 6), the rise in resistance can occur before crossing $H_y = 0$, which as is evident from the higher switching field (larger than the measured coercive fields of approximately 500 Oe for LPCMO thin films), may result from a hysteretic first-order phase change from CDI to FMM. We also note that the shape and size of the TMR peaks differs for each cooling cycle, as dictated by a dynamic phase-separated state. In fact, during some temperature cycles, we do not observe any TMR. The asymmetric TMR peaks observed at 51 K (black, centermost curve) and 52 K (fourth from bottom, blue curve), which were often seen in our measurements, may result from a unidirectional magnetic anisotropy and exchange bias at the interface between the antiferromagnetic COI tunnel barriers and FMM regions, as previously studied for bulk phase-separated manganites.[25] The presence of exchange bias between the insulating and FMM regions provides evidence that the tunneling is across the antiferromagnetic COI phase, rather than the paramagnetic CDI phase (see Sec. III C). Finally, we note peculiar mangetoresistance steps in Fig. 6 which are approximately, $R = 0.5$ kΩ in size. The origin of these steps is not yet clear, though given the microscopic size of the tunnel junctions formed, it may be a manifestation of the Barkhausen effect which results from the pinning of domain walls at defects in microscopic magnetic elements.[26] Alternatively, it may be related to incremental changes in spin canting within the insulating barrier or at the barrier-FMM interface.

3. Magnetoresistance for $T_G > T$ (Insulating domain walls)

Below T_G, the region in Fig. 2 corresponding to the high-resistance supercooled state, TMR was not observed since the sample is predominantly FMM (Ref. 19) upon ap-

plication of a field. In unpatterned LPCMO thin films which are also subject to tensile substrate-induced strain, the samples are fully ferromagnetic below T_G while in unstrained bulk LPCMO samples the COI phase remains robust down to low temperatures coexisting with CDI and FMM phases. However, for $T<T_G=48$ K, as in the parent compound $Pr_{0.67}Ca_{0.33}MnO_3$, the COI phase is metastable in applied magnetic fields and highly canted (very nearly ferromagnetic).[27] Doping half the Pr sites in $Pr_{0.67}Ca_{0.33}MnO_3$ with La which has the same valence as Pr but larger ionic radius (giving LPCMO), increases the average Mn-O-Mn bond angle (i.e., reducing lattice distortions which result from Pr doping[28]). The increased Mn-O-Mn bond angle increases the tolerance factor, thus increasing the overlap between the O 2_p and Mn e_g orbitals and making the metallic state energetically favorable. In like manner, the slight substrate-induced tensile strain further increases the Mn-O-Mn bond angle toward 180° in thin films, thus making the metallic state energetically more favorable than phase separation at low temperatures. Thus unpatterned thin films grown on (011) $NdGaO_3$ substrates are fully FMM at low temperatures.

However, we showed previously[5] that in the narrow bridges patterned from strained LPCMO thin films, the supercooled state consists of thin insulating regions that are stabilized at the ferromagnetic domain boundary, a phenomenon related to the reduced dimensions of the sample. We also showed evidence of direct electron tunneling across the insulating regions stabilized at the ferromagnetic domain boundary, i.e., the novel insulating stripe domain walls.[5,29,30] Upon application of a field, the insulating domain walls,[5] which act like tunnel junctions and comprise the remaining metastable insulating phase, are extinguished as spins in neighboring domains align resulting in sharp resistance drops and a uniform ferromagnetic region spanning the entire bridge. Thus TMR, which requires stable tunnel junction barriers, is never observed within this temperature region.

C. Magnetotransport across COI and CDI phases

The magnetoresistance data presented thus far on the patterned bridges allows us to speculate on the nature of the intrinsic insulating phases present within each temperature range. Summarizing from previous sections, in bulk samples the COI phase forms within the PI/CDI background near 240 K and remains robust down to low temperatures for $La_{0.275}Pr_{0.35}Ca_{0.375}MnO_3$ bulk crystals.[14,15] The insulator-to-metal transition in these samples occurs mainly from the CDI phase while the COI phase remains robust down to low temperatures. Also, $R(T)$ measurements show a clear feature at the PI to COI transition. In our case, for the $La_{0.33}Pr_{0.33}Ca_{0.33}MnO_3$ films grown on NGO substrates, no resistivity feature typical of the COI phase transition is observed near T_{CO} during cooling and the unpatterned samples are fully ferromagnetic metallic at low temperatures. We thus suspect that the COI phase is partially suppressed due to substrate-induced tensile strain as described in Secs. I and III. In the bulk parent compound $Pr_{0.67}Ca_{0.33}MnO_3$, the COI phase becomes highly canted, nearly ferromagnetic and

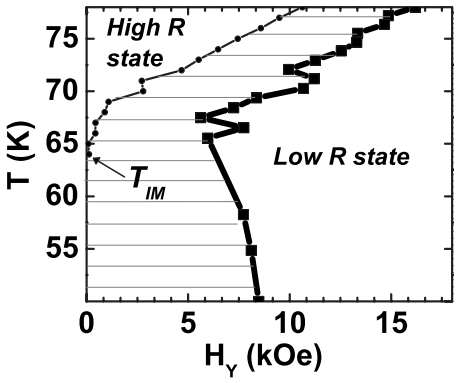

FIG. 7. A T-H_y phase diagram summarizing the low- and high-resistance switching fields, similar to bulk (Ref. 13) and thin-film (Ref. 19) T-H phase diagrams. The bold boundary (right) indicates the switching field from the high- to low-R state for increasing field while the thinner boundary (left) is for an increase back to a high-R state for decreasing field. At low enough temperature, the FMM phase is energetically favorable while the insulating phase is metastable in an applied magnetic field, and thus the sample remains in the low-R state for all increasing and decreasing field sweeps following the initial field increase (see Fig. 5).

metastable in magnetic fields as small as ≈2.1–4.5 kOe below about 70 K.[13] [In contrast, for $Pr_{0.625}Ca_{0.375}MnO_3$ the COI phase becomes metastable at temperatures around 30 K (Ref. 13)]. Hence, any COI phase present below T_G in the LPCMO films employed in this study is expected to be metastable in applied fields of the same range or perhaps lower given the substrate-induced strain. We further suspect that the metastable, canted antiferromagnetic COI phase is the CDI phase observed in previous work.[14,15]

Figure 7 shows a T-H phase diagram which summarizes the magnetoresistance properties of a discrete number of insulating states present in the 0.6-μm-wide LPCMO bridge for $78\ \mathrm{K} > T > 50\ \mathrm{K}$. The phase diagram qualitatively matches the unpatterned thin-film T-H diagram.[19] The wider and thinner lines mark the critical magnetic (switching) fields between the high- and low-resistance state for increasing and decreasing fields, respectively. The diagram illustrates the change in phase fraction and energy balances with lowering temperature. As the temperature is lowered, the FMM phase becomes energetically favorable thus requiring lower fields for a switch from a high- to low-resistance state. Below T_{IM}, the insulating phase is metastable in an applied magnetic field and the samples remain in the low-resistance state after an initial field sweep. The magnetic field required for the insulator-metal transition increases with lowering temperatures due to decreasing thermal fluctuations.

For temperatures between T_{CO} and T_{IM}^0, the sample is in a predominantly insulating state consisting of the CDI and COI phases. In this range the measured magnetoresistance for both the unpatterned thin films and patterned bridges is qualitatively the same. Between T_{IM}^0 and T_{IM}, small ferromagnetic droplets within the CDI regions coexist with the COI regions. In this temperature range (see Sec. III B 1), upon application of a magnetic field (< 20 kOe) there is a hysteretic transition to a low-resistance state, though full metallic resistivity values are not achieved. The fields applied in

our experiment are not high enough to melt the COI phase and we thus speculate that the high- and low-resistance states represent a hysteretic insulator-metal transition between the CDI and FMM phases with similar free energies. Any remaining COI phase is responsible for the larger than metallic resistance values observed in the lower-resistance state. With decreasing temperature, the FMM phase becomes energetically favorable, accounting for the lower switching fields and larger hysteresis observed in Fig. 3.

For $T_{IM} > T > T_G$, any remaining CDI phase is metastable in small fields $\sim$1000 Oe and the application of a magnetic field results in a transition to a low-resistance state. However, metallic resistivity values as before, are not achieved and the remaining insulating regions within the bridge are most likely of the COI phase. For fields $\leq$20 kOe, TMR is observed across the remaining COI regions separating FMM regions with different coercive fields. The fact that TMR is observed across the remaining COI phase is further corroborated by the observation of asymmetric TMR peaks (a signature of exchange bias).

As the temperature is reduced below T_G, the remaining COI regions become metastable (as for the parent compound $Pr_{0.625}Ca_{0.375}MnO_3$), and stabilize at the ferromagnetic domain boundaries as a result of the reduced dimensions of the sample. It is possible that the COI phase has completely converted to CDI at these low temperatures and stabilizes strain between two ferromagnetic domains of different magnetic polarization, thus resulting in the insulating domain walls observed[5] and predicted in such a scenario.[29] The smaller sample size essentially modifies the balance between long-range Coulomb interactions, the magnetic anisotropy, surface tension between the phases, etc.[30] Thus, at low temperatures, magnetic fields on the order of the LPCMO coercive field give rise to colossal drops in resistance and metallic resistivities are realized in the sample.[5]

Our data support the notion that the CDI phase, which is metastable[15] in magnetic fields forms the boundary[14] between the FMM and COI regions, and may have a canted antiferromagnetic (nearly FMM) structure, as discussed in the first paragraph of this section. In this picture, as the sample temperature is lowered, the FMM phase becomes more favorable, at the expense of the COI phase. The COI phase shrinks with CDI regions remaining constant at the boundary. Thus, below T_G, when the COI regions have completely changed to CDI which stabilize strain at the FM domain boundaries, a magnetic field on the order of the LPCMO coercive field induces a phase transition of the remaining CDI regions to FMM as the neighboring FMM domain spins align.

IV. CONCLUSION

In summary, temperature-dependent magnetoresistance measurements across narrow manganite bridges have allowed us to probe the formation and dynamics of the phase-separated regions in LPCMO on the nanometer length scale. At temperatures which define the onset of large-scale phase separation, we have observed abrupt and colossal low-field resistance changes which are anisotropic with respect to applied field. Further, within the dynamic phase-separated temperature range we have observed evidence of thin COI tunnel barriers which span the width of the narrow manganite bridges, separating adjacent ferromagnetic regions. The observation of reproducible TMR between high (antiparallel) and low (parallel) states confirms spin-polarized tunneling across the intrinsic COI tunnel barriers. Pronounced anisotropies and steps in both the CMR and TMR measurements highlight signatures of various microscopic phenomenon that occur during phase separation (i.e., exchange bias, shape anisotropy, and spin canting) which can be difficult to clearly identify in bulk sample measurements. From a technological perspective, control and manipulation of intrinsic tunnel barriers may prove useful for nanoscale spintronic applications in systems exhibiting similar phase separation at room temperature.

ACKNOWLEDGMENTS

This work was supported by the U.S. National Science Foundation under Grants No. 0704240 (A.F.H.) and No. 0804452 (A.B.).

*Corresponding author; afh@phys.ufl.edu

[1] H. Y. Hwang, S-W. Cheong, N. P. Ong, and B. Batlogg, Phys. Rev. Lett. **77**, 2041 (1996).
[2] A. Gupta, G. Q. Gong, G. Xiao, P. R. Duncombe, P. Lecoeur, P. Trouilloud, Y. Y. Wang, V. P. Dravid, and J. Z. Sun, Phys. Rev. B **54**, R15629 (1996).
[3] N. D. Mathur, G. Burnell, S. P. Isaac, T. J. Jackson, B.-S. Teo, J. L. MacManus-Driscoll, L. F. Cohen, J. E. Evetts, and M. G. Blamire, Nature (London) **387**, 266 (1997).
[4] J. Sun, W. Gallagher, P. Duncombe, L. Krusin-Elbaum, R. A. Altman, A. Gupta, Y. Lu, G. Q. Gong, and G. Xiao, Appl. Phys. Lett. **69**, 3266 (1996).
[5] G. Singh-Bhalla, S. Selcuk, T. Dhakal, A. Biswas, and A. F. Hebard, Phys. Rev. Lett. **102**, 077205 (2009).
[6] H.-Y. Zhai, J. X. Ma, D. T. Gillaspie, X. G. Zhang, T. Z. Ward, E. W. Plummer, and J. Shen, Phys. Rev. Lett. **97**, 167201 (2006).
[7] Y. Yanagisawa, H. Tanaka, T. Kawai, and L. Pellegrino, Appl. Phys. Lett. **89**, 253121 (2006).
[8] T. Wu and J. F. Mitchell, Phys. Rev. B **74**, 214423 (2006).
[9] In bulk single crystals, temperature-dependent resistivity measurements reveal a discontinuity at the PI to COI transition temperature, which is not seen in our thin films. Since each phase has different lattice constants, it is thus possible that due to substrate-induced strain (which may be enhanced at low temperatures resulting from mismatched thermal coefficients), the PI to COI transition is suppressed and a much smaller portion of the sample undergoes a transition to the COI phase in thin-film form.
[10] V. Podzorov, B. G. Kim, V. Kiryukhin, M. E. Gershenson, and

S-W. Cheong, Phys. Rev. B **64**, 140406(R) (2001).
[11] L. Ghivelder and F. Parisi, Phys. Rev. B **71**, 184425 (2005).
[12] P. A. Sharma, S. B. Kim, T. Y. Koo, S. Guha, and S-W. Cheong, Phys. Rev. B **71**, 224416 (2005).
[13] Y. Tomioka, A. Asamitsu, H. Kuwahara, Y. Moritomo, and Y. Tokura, Phys. Rev. B **53**, R1689 (1996).
[14] H. J. Lee, K. H. Kim, M. W. Kim, T. W. Noh, B. G. Kim, T. Y. Koo, S.-W. Cheong, Y. J. Wang, and X. Wei, Phys. Rev. B **65**, 115118 (2002).
[15] V. Kiryukhin, B. G. Kim, V. Podzorov, S.-W. Cheong, T. Y. Koo, J. P. Hill, I. Moon, and Y. H. Jeong, Phys. Rev. B **63**, 024420 (2000).
[16] R. P. Rairigh, G. Singh-Bhalla, S. Tongay, T. Dhakal, A. Biswas, and A. F. Hebard, Nat. Phys. **3**, 551 (2007).
[17] M. Uehara, S. Mori, C. H. Chen, and S.-W. Cheong, Nature (London) **399**, 560 (1999).
[18] L. Zhang, C. Israel, A. Biswas, R. Greene, and A. de Lozanne, Science **298**, 805 (2002).
[19] T. Dhakal, J. Tosado, and A. Biswas, Phys. Rev. B **75**, 092404 (2007).
[20] D. Gillaspie, J. Ma, H.-Y. Zhai, T. Ward, H. M. Christen, E. Plummer, and J. Shen, J. Appl. Phys. **99**, 08S901 (2006).
[21] M. Ziese, Rep. Prog. Phys. **65**, 143 (2002).
[22] A. Biswas, M. Rajeswari, R. C. Srivastava, Y. H. Li, T. Venkatesan, R. L. Greene, and A. J. Millis, Phys. Rev. B **61**, 9665 (2000).
[23] S. Kumar, C. Mohapatra, and P. Majumdar, Europhys. Lett. **71**, 804 (2005).
[24] A. O. Sboychakov, A. L. Rakhmanov, K. I. Kugel', M. Yu. Kagan, and I. V. Brodsky, J. Exp. Theor. Phys. **95**, 753 (2002).
[25] D. Niebieskikwiat and M. B. Salamon, Phys. Rev. B **72**, 174422 (2005).
[26] C. Tsang and S. K. Decker, J. Appl. Phys. **52**, 2465 (1981).
[27] Y. Tomioka and Y. Tokura, *Metal-Insulator Phenomena Relevant to Charge/Orbital Ordering in Perovskite-Type Manganese Oxides* (Gordon and Breach Science, New York, 2000), Chap. 8, pp. 281–306.
[28] S.-W. Cheong and H. Hwang, *Ferromagnetism vs. Charge/Orbital Ordering in Mixed-Valent Manganites* (Gordon and Breach Science, New York, 2000), Chap. 7, pp. 237–280.
[29] G. C. Milward, M. J. Calderon, and P. B. Littlewood, Nature (London) **433**, 607 (2005).
[30] D. I. Golosov, Phys. Rev. B **67**, 064404 (2003).